



Published in final edited form as:

Eur Polym J. 2015 November 1; 72: 566–576. doi:10.1016/j.eurpolymj.2015.04.028.

Gelation characteristics, physico-mechanical properties and degradation kinetics of micellar hydrogels

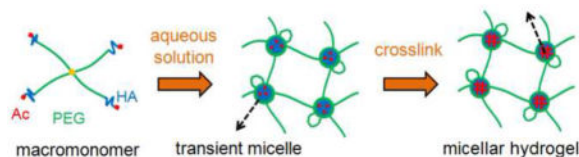
Seyedsina Moeinzadeh and Esmail Jabbari

Biomimetic Materials and Tissue Engineering Laboratory, Department of Chemical Engineering, University of South Carolina, Columbia, SC 29208, USA

Abstract

Due to their high water content and diffusivity of nutrients and biomolecules, hydrogels are very attractive as a matrix for growth factor immobilization and *in situ* delivery of cells to the site of regeneration in tissue engineering. The formation of micellar structures at the nanoscale in hydrogels alters the spatial distribution of the reactive groups and affects the rate and extent of crosslinking and mechanical properties of the hydrogel. Further, the degradation rate of a hydrogel is strongly affected by the proximity of water molecules to the hydrolytically degradable segments at the nanoscale. The objective of this review is to summarize the unique properties of micellar hydrogels with a focus on our previous work on star polyethylene glycol (PEG) macromonomers chain extended with short aliphatic hydroxy acid (HA) segments (SPEXA hydrogels). Micellar SPEXA hydrogels have faster gelation rates and higher compressive moduli compared to their non-micellar counterpart. Owing to their micellar structure, SPEXA hydrogels have a wide range of degradation rates from a few days to many months as opposed to non-degradable PEG gels while both gels possess similar water contents. Furthermore, the viability and differentiation of mesenchymal stem cells (MSCs) is enhanced when the cells are encapsulated in degradable micellar SPEXA gels compared with those cells encapsulated in non-micellar PEG gels.

Graphical Abstract



Keywords

Micellar hydrogel; Aliphatic hydroxy acid chain extension; Cell encapsulation; Gelation; Degradation; Elasticity

Corresponding author: Esmail Jabbari, Ph.D., Professor of Chemical and Biomedical Engineering, Swearingen Engineering Center, Rm 2C11, University of South Carolina, Columbia, SC 29208, Tel: (803) 777-8022, Fax: (803) 777-0973, jabbari@mailbox.sc.edu.

Publisher's Disclaimer: This is a PDF file of an unedited manuscript that has been accepted for publication. As a service to our customers we are providing this early version of the manuscript. The manuscript will undergo copyediting, typesetting, and review of the resulting proof before it is published in its final citable form. Please note that during the production process errors may be discovered which could affect the content, and all legal disclaimers that apply to the journal pertain.

1. Introduction

Hydrogels are hydrophilic polymeric networks that retain a significant fraction of water in the equilibrium state without dissolving. Owing to their high water content and high permeability to small nutrient molecules and large proteins, hydrogels are used as a carrier for delivery of cells to the site of regeneration in cell based therapies and tissue regeneration [1–5]. In that approach after injection and *in situ* hardening, the gel is gradually degraded to provide new volume for neo-tissue formation and replacement by the patient's own tissue [2]. Natural hydrogels like collagen, chitosan, and alginate as well as synthetic polyethylene glycol (PEG) and polypeptide gels are used as a carrier in stem cell delivery in regenerative medicine [6–13]. Neural stem cells (NSCs) encapsulated in alginate gels differentiated into neuronal lineages only in gels with an elastic modulus similar to that of brain tissue (100–1000 Pa) [14]. Likewise natural and synthetic hydrogels like PEG [15], collagen [16], chitosan [17], mixture of PEG and agarose [18], and mixture of hyaluronic acid and chitosan [19] have been used as a matrix for cell delivery in cartilage regeneration. Tissue engineered constructs require composite, multi-phasic, micro-patterned gels with a wide range of elasticity and degradability to support neurogenesis, vascularization, and structural stability. As an example, osteogenesis requires a highly elastic and slowly degrading matrix whereas a compliant fast-degrading matrix is essential for vasculogenesis [20–22]. Aside from biocompatibility, hydrogels used in cell delivery should have fast gelation kinetics to reduce the exposure of cells to reactive macromers and low molecular weight initiators, provide a wide range of elasticity, and degrade concurrent with tissue formation [6]. In that regard, synthetic macromonomers and more specifically the inert non-immunogenic PEG macromonomers generate hydrogels with a wide range of elasticity and stiffness [23,24] and the extent of interaction and adhesion of the encapsulated cells with the matrix can be controlled by conjugation of integrin- and heparin-binding peptides to the gel [25,26]. However, most synthetic hydrogels like PEG, polyvinyl alcohol (PVA), polyacrylamide (PAM), and poly(hydroxyethyl methacrylate) (PHEMA) are non-degradable and their use as a cell delivery matrix is limited by their persistence at the site of delivery, thus limiting the rate of tissue regeneration [27–29]. Co-polymerization of hydrophilic macromers with degradable hydrophobic monomers generates macromonomers which form micellar structures in aqueous solution [30–32]. These micellar structures affect the proximity of water molecules to the hydrolytically degradable segments of the copolymer chains at the nanoscale leading to a noticeable change in gelation kinetics, elasticity, and degradation of the hydrogel [32]. In this work we review the unique properties of micellar hydrogels specifically those based on star polyethylene glycol (PEG) macromonomers chain extended with short aliphatic hydroxy acid (HA) segments (SPEXA hydrogels) with respect to water-copolymer interaction, water content, gelation kinetics, elasticity, degradation, and cell-matrix interaction.

2. Physically versus covalently bonded micellar gels

It is well known that surfactant-like amphiphilic diblock copolymers such as PEG-polypropylene oxide (PEG-PEO), PEG-poly(lactide) (PEG-PLA), and PEG-poly(lactide-co-glycolide) (PEG-PLGA) form micelles in aqueous solution at low concentrations and undergo physical gelation at high concentrations [33,34]. Hydrogel formation by diblock

confinement of the crosslinking reaction to the micellar phase imparts special properties to the hydrogel with respect to gelation kinetics, elasticity, water content, and cell-matrix interactions in cell encapsulation [32]. To test that, we synthesized a series of degradable covalently crosslinkable micelle-forming macromonomers by chain extension of star 4-arm PEG macromers with short aliphatic hydroxy acid (HA) segments including L-lactide (L), glycolide (G) and ϵ -caprolactone (C) followed by termination of the arms with a reactive acrylate (Ac) group (SPEXA macromonomer with X=L, G or C) (Fig. 1) [30,31,51–53]. The SPELA, SPEGA and SPECA macromonomers are hereafter denoted by L, G and C, respectively. The star PEG acrylate without chain extension with HA is denoted by “w/o HA”. The length of the hydrophobic HA segment on each arm was relatively short (<5 HA monomers per arm) for the macromonomer to be soluble in aqueous solution [30,52]. Dissipative Particle Dynamics (DPD) simulations demonstrated that the hydrophobic segments of SPEXA macromonomers aggregated to form micelles in the hydrogel precursor solution [30,31,52]. The hydrophobic HA segments and Ac units formed the micelles’ core whereas the hydrophilic PEG segments formed the corona (Fig. 1) [30,31,52]. The size, aggregation number (number of macromonomers per micelle) and number density of micelles depended on the number of HA monomers per arm (m). According to the simulation results, core radius of the G, L and C micelles increased from 0, 9 and 11 Å to 22, 23 and 24 Å, respectively, when m increased from 1 to 4 [30]. The G macromonomers did not form micelles when m was 1 whereas the more hydrophobic L and C macromonomers formed micellar structures even with just one monomer per macromonomer arm [30]. In addition, the average aggregation number of C micelles increased from 4 to 19 when m increased from 1 to 4 which was the highest aggregation number among the three macromonomers. The G macromonomer had the lowest aggregation number in the range of 0 to 14 as m increased from 1 to 4 [30]. A similar trend is reported for linear PEG-PLA copolymers with respect to micelle core size and aggregation number with increasing HA segment length [54]. The simulation results also showed that the SPEXA macromonomer concentration (in 5–30 wt% range) had a significant effect on size of the micelles [31].

3. Gelation kinetics and viscoelastic properties of micellar gels

The gelation kinetics and viscoelastic properties of physically or covalently crosslinked micellar gels was evaluated by rheometry. The frequency sweep tests on physically crosslinked micellar gels at temperatures slightly above the sol-gel transition demonstrated that the micellar gel precursor solutions maintained a viscous response at low frequencies and an elastic response at high frequencies [38]. The shear storage (G') and loss (G'') moduli increased with different power law dependencies ($G' \sim f^2$, $G'' \sim f$) at low frequencies and intersected at $f_{G'=G''}$ [38]. The rate of increase of G' and G'' became slower and relatively independent of frequency at frequencies higher than $f_{G'=G''}$ where $G' > G''$ [38]. The residence time of an inter-micellar bridge (τ) is given by [38]

$$\tau = \frac{1}{2\pi f_{G'=G''}} \quad (1)$$

At time scales well below τ or at temperatures well above the sol-gel transition, the transient bridges act as permanent crosslinks and contribute to the gel's elasticity [32,38]. Since τ increases with the extent of hydrophobicity and length of the hydrophobic block, the stability of the transient micellar network increases with the above-mentioned factors of the macromonomer [32,38].

The gelation kinetics of covalently crosslinked micellar gels depend on several factors including the concentration and distribution of crosslinkable groups and initiator concentration [30,31,52,53]. The gelation time of L macromonomers with respect to the concentration of UV photo-initiator is shown in Fig. 2a. As the initiator concentration was increased from 0.08 to 0.80 wt%, gelation time of L macromonomers decreased from 200 ± 9 to 42 ± 2 s [52], respectively. A decrease in the gelation time with increasing photo-initiator concentration was attributed to an increase in the propagation rate of crosslinking by [55]

$$R_p = K_p [AC] \left[\frac{\phi \varepsilon I_0 \delta [I]}{K_t} \right]^{1/2} \quad (2)$$

where K_p and K_t are the rate constants for chain propagation and termination, respectively, $[AC]$ is the concentration of unreacted acrylates, ϕ is the initiation efficiency, ε is the molar extinction coefficient, I_0 is the intensity of incident radiation, δ is the sample thickness, and $[I]$ is the photo-initiator concentration. According to eq. 2, the propagation rate of crosslinking for L macromonomers increased with increasing initiator concentration which led to a decrease in gelation time (Fig. 2a). The rate of photo-activation of acrylates depended on the proximity of initiator molecules to acrylate groups. The inset in Fig. 2a shows a simulated distribution of photo-initiator beads (pink color) within the core of L micelles (brown and red colors represent lactide and acrylate beads, respectively). The simulation images indicate that 98% of the photo-initiator beads partitioned into the hydrophobic core of the micelles in the proximity of acrylates. Therefore, the crosslinking reaction was confined to the micellar phase in the SPEXA gel precursor solutions. The gelation time of SPEXA gels with respect to the concentration of reactive acrylate groups is shown in Fig. 2b. The gelation time of G hydrogels decreased from 128 to 60 s with increasing acrylate concentration from 0.02 to 0.13 mol/L, respectively (Fig. 2b). The gelation time of L and C gels ranged from 64 to 28 s and from 77 to 30 sec, respectively, which were significantly lower than the G gel. A decrease in gelation time with increasing the concentration of acrylates was attributed to an increase in the rate of propagation reaction (see eq. 2). Based on simulation results, the propensity for micelle formation decreased and the fraction of acrylate groups in the aqueous solution (free from the micelle core) increased when HA type was changed from C to L and G [30]. As a result, a significant part of the crosslinking reaction occurred in the aqueous phase for the less hydrophobic G macromonomers whereas a significant part of the crosslinking reaction occurred in the micellar phase for the L and C macromonomers. Therefore, the L and C micellar gels had a faster crosslinking rate and shorter gelation time compared to the G gels [30]. The slightly lower gelation time of the L gel compared to that of C gel was attributed to the more branched structure of the L monomer than C, hence higher residence time of

acrylate end groups within the micelle's cores and faster crosslinking reaction for the L macromonomers compared with C [56]. The effect of number of HA monomers per macromonomer (m) on the gelation time of SPEXA macromonomers is shown in Fig. 2c. The gelation time of G, L and C macromonomers decreased from 150 s to 61, 28 and 34 s, respectively, with increasing m from 0 to 3 [30]. The initial sharp decrease in gelation time of SPEXA macromonomers was attributed to a change in the distribution of reactive Ac groups concurrent with micelle formation. According to simulation results (Fig. 2d), the Ac beads (The chemical structures of the beads are shown in Fig. 2e) were uniformly distributed in the aqueous solution in the absence of HA segments (red beads in Fig. 2d-w/o HA) whereas the Ac beads were positioned in the core of the micelles concurrent with micelle formation in the G, L and C gel precursor solutions (Fig. 2d). The Ac groups were localized within the micelles' core which decreased gelation time with increasing m for all three HA types (Fig. 2c). The simulation results also showed that the proximity of Ac groups in the SPEXA gel precursor solution increased with changing the HA type from G to L or C (at the same m) concurrent with the formation of larger micelles. These results were consistent with the shorter experimental gelation times for the L and C macromonomers compared to G [30].

The effect of acrylate concentration on the compressive modulus of SPEXA hydrogels is shown in Fig. 3a. The compressive modulus of C, G and L gels increased from 50, 50, and 20 kPa to 480, 710 and 460 kPa, respectively, with increasing the Ac concentration from 0.04 to 0.13 mol/L (Fig. 3a). The elastic response of the hydrogels can be explained using the rubber elasticity theory developed by Treloar and Flory [57] and modified by Peppas and Merrill [58]. According to that theory, the elastic modulus of a crosslinked network is [59]

$$E = \nu_E RT \quad (3)$$

where ν_E , R and T are the density of elastically active chains, the gas constant and the absolute temperature, respectively. The density of crosslinks increased with increasing the acrylate concentration in the gel precursor solution. Further, the probability of forming elastically inactive loops by the reaction between two acrylates on the same macromonomer decreased with increasing the acrylate concentration [4,42]. Therefore, the compressive modulus of the SPEXA gels steadily increased with increasing the acrylate concentration. The effect of m on the compressive modulus of SPEXA hydrogels is shown in Fig. 3b. The compressive modulus of L, C, and G gels increased significantly from 330 to 390, 420 and 620 kPa, respectively, as m increased from 0 to 2.9 (2.8 for C). The above-mentioned increase was related to a change in the nanostructure of the gel as well as the acrylate distribution concurrent with the formation of micelles [30,31]. As shown in Fig. 3c, the number density of L micelles decreased and the number of inter-micellar bridges per micelle increased with increasing m . The residence time of transient inter-micellar bridges within the micelles (τ) is proportional to [56]

$$\tau \sim \gamma m^{2/3} \quad (4)$$

Where γ is the effective interfacial tension between the micelle's core and aqueous solution. Therefore, the residence time of the inter-micellar bridges increased with increasing m concurrent with an increase in the number of transient bridges per micelle. Thus, the probability of a crosslinking reaction in the micelles' core and the conversion of a transient bridge to a permanent bridge increased with increasing m . The probability of intra-molecular reaction (loop formation) in the free radical crosslinking reaction of multi-functional macromonomers is given by [60]

$$\Psi = 1 - \frac{1}{\exp\left(\frac{A}{[AC]r_0 l^2}\right)} \quad (5)$$

Where $[AC]$ is the local concentration of acrylates, r_0 is the average distance between the double bonds on macromonomers, l is the statistical length of a repeating unit and A is a constant ($A = 3/4\pi N_A$ where N_A is Avogadro's number). According to eq. 5, the probability of loop formation decreased with increasing m due to an increase in the local concentration of acrylates as described earlier. Altogether, the net effect of increasing m in the SPEXA macromonomer is an increase in the probability of formation of permanent inter-micellar bridges and a decrease in the probability of formation of elastically inactive loops. Therefore based on the theory of rubber elasticity, the compressive modulus of SPEXA gels increased with increasing m (Fig. 3b).

4. Swelling of micellar gels

The degree of swelling (or water content) of a hydrogel is typically controlled by two opposing forces, namely the thermodynamic force of mixing between the polymer and water and the elastic force of extending polymer chains [57]. The force of mixing tends to increase the water content of the gel by attractive interactions between water molecules and the network chains [57]. The elastic force of extending polymer chains on the other hand tends to decrease the water content of the gel due to a change in polymer chain conformation from an entropically more favorable random coil to a less favorable extended conformation. Several factors including molecular weight, hydrophobicity, functionality and flexibility of the macromonomers, degree of crosslinking, nanostructure of the gel and temperature affect hydrogel swelling [61,62]. Specifically, the hydrogel swelling decreases with increasing hydrophobicity of the chains and crosslink density by influencing the force of mixing and the elastic force of the chains, respectively [58]. The effect of acrylate group concentration on the swelling of micellar SPEXA gels is shown in Fig. 4a. The swelling ratio of C, L and G gels decreased from 710 to 300%, 730 to 340% and 830 to 430%, respectively, when the acrylate concentration increased from 0.02 to 0.13 mol/L [51]. A decrease in the swelling ratio of SPEXA gels with increasing acrylate concentration was attributed to an increase in crosslink density. The swelling of hydrogels decreased slightly concurrent with increasing the hydrophobicity of HA segments from G to L and C at the same acrylate concentration. The effect of m on the water content of SPEXA gels is shown in Fig. 4b. The bulk water content of SPEXA gels ranged between 78% to 83% and m did not have a statistically significant effect on the water content of hydrogels. The data in Fig. 4b implies that the chain extension of star PEG macromonomers with short HA segments, due to the formation

of micellar structures at the nanoscale, did not negatively affect the water content of SPEXA hydrogels.

5. Degradation of micellar gels

Although hydrogels provide enormous flexibility in controlling the cell microenvironment, their use in regenerative medicine is limited by their persistence in the site of regeneration [6]. Therefore, hydrogels for tissue engineering applications should be degradable with a rate corresponding to that of ECM production and remodeling [6]. The role of matrix degradation on the fate of encapsulated cells has been investigated previously. C2C12 mouse myoblast cells encapsulated in a degradable alginate gel had lower proliferation and higher extent of myotube formation compared to those encapsulated in a non-degradable gel [63]. Similarly, MSCs encapsulated in a non-degradable hyaluronic acid gel underwent adipogenic differentiation whereas those encapsulated in a degradable gel differentiated to the osteogenic lineage [64]. The rate of hydrogel degradation can also affect tissue morphogenesis. For instance, blood vessel formation and angiogenesis require a relatively fast (few days) degrading gel whereas mineralization and osteogenesis require a relatively slow (few weeks) degrading gel [20–22]. Therefore, there is a need to develop hydrogels with tunable degradation in order to regenerate complex tissues with many cell types.

Synthetic hydrogels can be made degradable with incorporation of enzymatic, hydrolytic or photolytically degradable segments in the macromonomer chains or crosslinkers [65]. Copolymerization of non-degradable hydrophilic macromers with degradable lactide and glycolide blocks has been used to impart degradability and control the water content of PEG hydrogels [4,66] but solubility of the copolymer in the aqueous gel precursor solution for cell encapsulation decreased dramatically with increasing the length of lactide blocks [53]. Hydrogels synthesized from PEG and ϵ -caprolactone co-polymers are shown to be hydrolytically degradable, but the degradation rate is limited by the hydrophobicity and phase separation of ϵ -caprolactone segments in solution [67]. In addition to poly(aliphatic hydroxy acids), other hydrolytically degradable polymers including poly(ester amides) [68], polyphosphoesters [69,70], poly(amino-ester urethanes) [71] are used to synthesize degradable hydrogels. Photodegradable hydrogels are synthesized by incorporation of nitrobenzyl ether-derived moieties in PEG based hydrogels [72]. Remarkably, the SPEXA macromonomers chain extended with short HA segments generate micellar hydrogels with a wide range of degradation rates [30,51,52]. Owing to the micellization of hydrophobic segments, the degradation of SPEXA gels can be tuned to a particular application from a few days to a few weeks, few months, and many months by changing hydrophobicity and length of the HA segments [30,51,52]. The mass losses of SPEXA hydrogels in a narrow range of m values (1.6 $\leq m \leq$ 1.8) are compared in Fig. 5a. While the PEG hydrogel without HA (red curve in Fig. 5a) had only 6% mass loss after 6 weeks of incubation, the C hydrogel lost 20% mass in 6 weeks and the G and L hydrogels completely degraded in 3 days and 5 weeks, respectively. Based on simulation results, the differences in hydrophobicity of HA monomers and number of hydrolytically-degradable ester groups per HA monomer contributed to the measured wide range of degradation rates for SPEXA hydrogels (Fig. 5a) [30]. The G and L macromonomers had 2 ester groups per HA monomer whereas the C macromonomer had one ester group. In addition, the hydrophilicity of HA monomers which

affected their proximity to water molecules, increased from C to L and G (Fig. 5c). As a result, the G hydrogel with 2 ester groups per HA monomer and highest proximity of ester moieties to water molecules had the highest degradation rate whereas the C hydrogel with one ester group per HA monomer and ester moieties furthest away from water molecules had the lowest degradation rate (Fig. 5a). The effect of m on mass loss of the L hydrogel was bimodal as shown in Fig. 5b. The mass loss of 20 wt% L gels increased from 6 to 37, 80 and 100% after 28 days of incubation when m increased from zero to 0.8, 1.7 and 2.9, respectively. Then, the mass loss decreased from 100 to 87% with increasing m from 2.9 to 3.7. The bimodal effect of m on mass loss of SPEXA gels was attributed to the formation of large micelles for $m > 3$ with reduced proximity of water molecules to ester groups in the micelles' core (Fig. 5b). The formation of micelles did not significantly affect the bulk water content of the SPEXA gels (Fig. 4b). However, the hydrophobic core of the micelles repelled water molecules, which decreased their proximity to the ester groups, leading to a reduction in the rate of degradation of SPEXA gels at high m values and a transition from surface (controlled by the number of ester groups) to bulk (dominated by the water content of micelles) degradation [30].

6. Cell-matrix interactions in micellar gels

Cell-matrix interactions within a cell-laden hydrogel play a central role in regulating cell function [73,74]. In the natural extracellular matrix (ECM), cell adhesive proteins such as laminin and fibronectin bind to integrin cell surface receptors to regulate cell adhesion, migration, and differentiation [73,75,76]. Further, soluble proteins or tethered growth factors, present in the ECM, modulate proliferation, migration and differentiation of the cells [77]. Therefore, synthetic hydrogels should be modified with bioactive ligands for optimal cell-matrix interaction [78]. In that regard, the viability of human MSCs was significantly higher in a PEG gel conjugated with cell-adhesive arginine-glycine-aspartic acid (RGD) peptide as compared with that with no peptide [79]. Human MSCs seeded on PEG hydrogels modified with RGD and an osteoinductive BMP-2 protein-derived KIPKASSVPTELSAISTLYL peptide showed 5- and 12-fold increase in ALP activity and calcium content after 14 and 21 days of incubation, respectively [25]. We have previously shown that the viability of MSCs encapsulated in the micellar PEG gels and their differentiation to the osteogenic lineage are significantly enhanced by the incorporation of RGD peptide and BMP-2 protein or peptide in the hydrogel matrix [52,80]. In addition, the micellar nature of the gel affects cell viability and function. The simulated fraction of initiator molecules (the fraction not partitioned to the micelles' core) in the L hydrogel precursor solution decreased from 100% to 7.4, 3.3 and 2% as m increased from 0 to 1, 2 and 3, respectively (Fig. 6a). The partition of initiator molecules to the core limited the gelation reaction to the micelle phase, thus reducing the cytotoxic effect of low molecular weight initiator molecules on the encapsulated cells. Cell culture experiments showed that the viability of human MSCs after 2 days of encapsulation in the micellar L and C gels was significantly higher than those encapsulated in the non-micellar PEG gel [30]. Since the water content of micellar gels was similar to the non-micellar gel (w/o HA gel in Fig. 4b) and the toxic effect of the initiator was significantly lower, the viability of MSCs encapsulated in the micellar PEG was higher than the non-micellar gels. The osteogenic

differentiation of human MSCs encapsulated in the SPEXA gels (20 wt% and $m=1.7$) was evaluated by measuring alkaline phosphatase (ALP) activity (Fig. 6b) and calcium content (Fig. 6c) with incubation in osteogenic medium over 28 days. The G gel due to its relatively fast degradation was not used for MSC encapsulation. The ALP activity of MSCs encapsulated in the L, C and w/o HA gels increased from day 7 to 14 and then decreased from day 14 to 28. The peak in ALP activity corresponded to the initiation of osteogenesis as previously reported [25,31]. The ALP activity of MSCs encapsulated in the degradable L or C hydrogels at day 14 was significantly higher than those encapsulated in the non-degradable w/o HA gel. MSCs encapsulated in the L hydrogel had a higher ALP activity after 14 days compared to those in the C hydrogel. The calcium content of the encapsulated MSCs had an increasing trend with time over 28 days of incubation. The calcium content of MSCs encapsulated in the L gel, with ~80% mass loss after 28 days, was significantly higher than those in the C gel with ~20% mass loss. The calcium content of MSCs encapsulated in the L or C gel was higher than those in the non-degradable w/o HA gel after 28 days of incubation. The micellar SPEXA gels supported viability and differentiation of human MSCs to the osteogenic lineage. The SPEXA gels with high water content, tunable degradation, low gelation time, and adjustable stiffness can be used for differentiation of stem cells to other cell types as soft and fast-degrading SPEXA gels support vasculogenic differentiation of co-encapsulated MSCs and endothelial progenitor cells (EPCs) [51].

7. Conclusion

The formation of micellar structures in the aqueous solution of acrylated star PEG macromonomers chain extended with short aliphatic hydroxy acid (HA) segments (SPEXA) decreased gelation time and exposure time of encapsulated cells to the toxic polymerization photo-initiator. As a result of micelle formation, the degradation rate of SPEXA hydrogels was tunable from a few days to a few weeks, a few months, and many months by changing the HA monomer or varying the length of HA segment while maintaining a relatively constant water content. The compressive modulus of the micellar SPEXA hydrogels ranged from 5 to 700 kPa. The viability and osteogenic differentiation of encapsulated human MSCs was significantly higher in the micellar SPEXA hydrogels compared to the non-micellar PEG gel. Micellar hydrogels with a wide range of physico-mechanical properties are potentially useful as cell carriers in regeneration of living tissues from the relatively soft nerve and vascular tissues to stiff skeletal tissues.

Acknowledgments

This work was supported by research grants to E. Jabbari from the National Science Foundation under Award Numbers DMR1049381, IIP-1357109, and CBET1403545. Research reported in this publication was supported by the National Institute of Arthritis and Musculoskeletal and Skin Diseases of the National Institutes of Health under Award Number AR063745. The content is solely the responsibility of the authors and does not necessarily represent the official views of the National Institutes of Health. This work was also supported by the Arbeitsgemeinschaft Fur Osteosynthesefragen (AO) Foundation under Grant Number C10-44J, and the University of South Carolina VP Office for Research under Grant Number 15510-E414.

References

1. Cheng YH, Yang SH, Su WY, Chen YC, Yang KC, Cheng WTK, Wu SC, Lin FH. Thermosensitive chitosan-gelatin-glycerol phosphate hydrogels as a cell carrier for nucleus pulposus regeneration: An in vitro study. *Tissue Eng Part A*. 2010; 16:695–703. [PubMed: 19769528]
2. Sarvestani AS, He XZ, Jabbari E. Viscoelastic characterization and modeling of gelation kinetics of injectable in situ cross-linkable poly(lactide-co-ethylene oxide-co-fumarate) hydrogels. *Biomacromolecules*. 2007; 8:406–415. [PubMed: 17253761]
3. Peppas, NA.; Lustig, SR. *Hydrogels in Medicine and Pharmacy. I. Fundamentals*. Boca Raton, FL: CRC Press; 2004. Solute diffusion in hydrophilic network structures.
4. Sarvestani AS, Xu W, He X, Jabbari E. Gelation and degradation characteristics of in situ photocrosslinked poly(l-lactid-co-ethylene oxide-co-fumarate) hydrogels. *Polymer*. 2007; 48:7113–7120.
5. Zhao LA, Weir MD, Xu HHK. An injectable calcium phosphate-alginate hydrogel-umbilical cord mesenchymal stem cell paste for bone tissue engineering. *Biomaterials*. 2010; 31:6502–6510. [PubMed: 20570346]
6. Cushing MC, Anseth KS. Hydrogel cell cultures. *Science*. 2007; 316:1133–1134. [PubMed: 17525324]
7. Perez RA, Kim M, Kim TH, Kim JH, Lee JH, Park JH, Knowles JC, Kim HW. Utilizing core-shell fibrous collagen-alginate hydrogel cell delivery system for bone tissue engineering. *Tissue Eng Part A*. 2014; 20:103–114. [PubMed: 23924353]
8. Hesse E, Hefferan TE, Tarara JE, Haasper C, Meller R, Krettek C, Lu LC, Yaszemski MJ. Collagen type I hydrogel allows migration, proliferation, and osteogenic differentiation of rat bone marrow stromal cells. *J Biomed Mater Res Part A*. 2010; 94A:442–449.
9. Wang LM, Rao RR, Stegemann JP. Delivery of mesenchymal stem cells in chitosan/collagen microbeads for orthopedic tissue repair. *Cells Tissues Organs*. 2013; 197:333–343. [PubMed: 23571151]
10. Huebsch N, Arany PR, Mao AS, Shvartsman D, Ali OA, Bencherif SA, Rivera-Feliciano J, Mooney DJ. Harnessing traction-mediated manipulation of the cell/matrix interface to control stem-cell fate. *Nature Mater*. 2010; 9:518–526. [PubMed: 20418863]
11. Chen Y, Pang XH, Dong CM. Dual stimuli-responsive supramolecular polypeptide-based hydrogel and reverse micellar hydrogel mediated by host-guest chemistry. *Adv Funct Mater*. 2010; 20:579–586.
12. Jonker AM, Lowik DWPM, van Hest JCM. Peptide- and protein-based hydrogels. *Chem Mater*. 2012; 24:759–773.
13. Yao MH, Yang J, Du MS, Song JT, Yu Y, Chen W, Zhao YD, Liu B. Polypeptide-engineered physical hydrogels designed from the coiled-coil region of cartilage oligomeric matrix protein for three-dimensional cell culture. *J Mater Chem B*. 2014; 2:3123–3132.
14. Banerjee A, Arha M, Choudhary S, Ashton RS, Bhatia SR, Schaffer DV, Kane RS. The influence of hydrogel modulus on the proliferation and differentiation of encapsulated neural stem cells. *Biomaterials*. 2009; 30:4695–4699. [PubMed: 19539367]
15. Roberts JJ, Bryant SJ. Comparison of photopolymerizable thiol-ene PEG and acrylate-based PEG hydrogels for cartilage development. *Biomaterials*. 2013; 34:9969–9979. [PubMed: 24060418]
16. Yuan T, Zhang L, Li KF, Fan HS, Fan YJ, Liang J, Zhang XD. Collagen hydrogel as an immunomodulatory scaffold in cartilage tissue engineering. *J Biomed Mater Res Part B Appl Biomater*. 2014; 102:337–344. [PubMed: 24000202]
17. Mirahmadi F, Tafazzoli-Shadpour M, Shokrgozar MA, Bonakdar S. Enhanced mechanical properties of thermosensitive chitosan hydrogel by silk fibers for cartilage tissue engineering. *Mater Sci Eng C Mater Biol Appl*. 2013; 33:4786–4794. [PubMed: 24094188]
18. DeKosky BJ, Dormer NH, Ingavle GC, Roatch CH, Lomakin J, Detamore MS, Gehrke SH. Hierarchically designed agarose and poly(ethylene glycol) interpenetrating network hydrogels for cartilage tissue engineering. *Tissue Eng Part C Methods*. 2010; 16:1533–1542. [PubMed: 20626274]
19. Park H, Choi B, Hu JL, Lee M. Injectable chitosan hyaluronic acid hydrogels for cartilage tissue engineering. *Acta Biomater*. 2013; 9:4779–4786. [PubMed: 22935326]

20. Chatterjee K, Lin-Gibson S, Wallace WE, Parekh SH, Lee YJ, Cicerone MT, Young MF, Simon CG. The effect of 3D hydrogel scaffold modulus on osteoblast differentiation and mineralization revealed by combinatorial screening. *Biomaterials*. 2010; 31:5051–5062. [PubMed: 20378163]
21. Henderson JA, He X, Jabbari E. Concurrent differentiation of marrow stromal cells to osteogenic and vasculogenic lineages. *Macromol Biosci*. 2008; 8:499–507. [PubMed: 17941111]
22. Chen YC, Lin RZ, Qi H, Yang YZ, Bae HJ, Melero-Martin JM, Khademhosseini A. Functional human vascular network generated in photocrosslinkable gelatin methacrylate hydrogels. *Adv Funct Mater*. 2012; 22:2027–2039. [PubMed: 22907987]
23. Karimi T, Barati D, Karaman O, Moeinzadeh S, Jabbari E. A developmentally inspired combined mechanical and biochemical signaling approach on zonal lineage commitment of mesenchymal stem cells in articular cartilage regeneration. *Integr Biol*. 2014; 7:112–27.
24. Yang X, Sarvestani SK, Moeinzadeh S, He X, Jabbari E. Three-dimensional engineered matrix to study cancer stem cells and tumorsphere formation: Effect of matrix modulus. *Tissue Eng Part A*. 2013; 19:669–84. [PubMed: 23013450]
25. He X, Ma J, Jabbari E. Effect of grafting RGD and BMP-2 protein-derived peptides to a hydrogel substrate on osteogenic differentiation of marrow stromal cells. *Langmuir*. 2008; 24:12508–12516. [PubMed: 18837524]
26. He X, Yang X, Jabbari E. Combined effect of osteopontin and BMP-2 derived peptides grafted to an adhesive hydrogel on osteogenic and vasculogenic differentiation of marrow stromal cells. *Langmuir*. 2012; 28:5387–5397. [PubMed: 22372823]
27. An DB, Kim TH, Lee JH, Oh SH. Evaluation of stem cell differentiation on polyvinyl alcohol/hyaluronic acid hydrogel with stiffness gradient. *J Tissue Eng Regen Med*. 2014; 8:346–347.
28. Guo P, Yuan YS, Chi FL. Biomimetic alginate/polyacrylamide porous scaffold supports human mesenchymal stem cell proliferation and chondrogenesis. *Mater Sci Eng C Mater Biol Appl*. 2014; 42:622–628. [PubMed: 25063162]
29. Sun L, Li D, Hemraz UD, Fenniri H, Webster TJ. Self-assembled rosette nanotubes and poly(2-hydroxyethyl methacrylate) hydrogels promote skin cell functions. *J Biomed Mater Res Part A*. 2014; 102:3446–51.
30. Moeinzadeh S, Barati D, Sarvestani SK, Karaman O, Jabbari E. Nanostructure formation and transition from surface to bulk degradation in polyethylene glycol gels chain-extended with short hydroxy acid segments. *Biomacromolecules*. 2013; 14:2917–2928. [PubMed: 23859006]
31. Moeinzadeh S, Jabbari E. Mesoscale simulation of the effect of a lactide segment on the nanostructure of star poly(ethylene glycol-co-lactide)-acrylate macromonomers in aqueous solution. *J Phys Chem B*. 2012; 116:1536–1543. [PubMed: 22236036]
32. Moeinzadeh, S.; Jabbari, E. Nanostructure formation in hydrogels. In: Bhushan, B., et al., editors. *Handbook of Nanomaterials Properties*. Berlin: Springer; 2014. p. 285-297.
33. Gil ES, Hudson SM. Stimuli-responsive polymers and their bioconjugates. *Prog Polym Sci*. 2004; 29:1173–1222.
34. Jeong B, Bae YH, Lee DS, Kim SW. Biodegradable block copolymers as injectable drug-delivery systems. *Nature*. 1997; 388:860–862. [PubMed: 9278046]
35. Huynh CT, Nguyen MK, Lee DS. Injectable block copolymer hydrogels: Achievements and future challenges for biomedical applications. *Macromolecules*. 2011; 44:6629–6636.
36. Riess G. Micellization of block copolymers. *Prog Polym Sci*. 2003; 28:1107–1170.
37. Henn DM, Wright RAE, Woodcock JW, Hu B, Zhao B. Tertiary-amine-containing thermo- and pH-sensitive hydrophilic aba triblock copolymers: Effect of different tertiary amines on thermally induced sol-gel transitions. *Langmuir*. 2014; 30:2541–2550. [PubMed: 24548271]
38. O'Lenick TG, Jin NX, Woodcock JW, Zhao B. Rheological properties of aqueous micellar gels of a thermo- and pH-sensitive aba triblock copolymer. *J Phys Chem B*. 2011; 115:2870–2881. [PubMed: 21370841]
39. Woodcock JW, Jiang XG, Wright RAE, Zhao B. Enzyme-induced formation of thermoreversible micellar gels from aqueous solutions of multiresponsive hydrophilic aba triblock copolymers. *Macromolecules*. 2011; 44:5764–5775.

40. Cohn D, Lando G, Sosnik A, Garty S, Levi A. PEO-PPO-PEO-based poly(ether ester urethane)s as degradable reverse thermo-responsive multiblock copolymers. *Biomaterials*. 2006; 27:1718–1727. [PubMed: 16310849]
41. Kim HK, Shim WS, Kim SE, Lee KH, Kang E, Kim JH, Kim K, Kwon IC, Lee DS. Injectable in situ-forming pH/thermo-sensitive hydrogel for bone tissue engineering. *Tissue Eng Part A*. 2009; 15:923–933. [PubMed: 19061427]
42. Sanson N, Rieger J. Synthesis of nanogels/microgels by conventional and controlled radical crosslinking copolymerization. *Polym Chem*. 2010; 1:965–977.
43. Willet N, Gohy JF, Lei LC, Heinrich M, Auvray L, Varshney S, Jerome R, Leyh B. Fast multiresponsive micellar gels from a smart abc triblock copolymer. *Angewandte Chemie Int Ed*. 2007; 46:7988–7992.
44. Holmes TC, de Lacalle S, Su X, Liu GS, Rich A, Zhang SG. Extensive neurite outgrowth and active synapse formation on self-assembling peptide scaffolds. *Proc Natl Acad Sci U S A*. 2000; 97:6728–6733. [PubMed: 10841570]
45. Kisiday J, Jin M, Kurz B, Hung H, Semino C, Zhang S, Grodzinsky AJ. Self-assembling peptide hydrogel fosters chondrocyte extracellular matrix production and cell division: Implications for cartilage tissue repair. *Proc Natl Acad Sci U S A*. 2002; 99:9996–10001. [PubMed: 12119393]
46. Zhang SG, Holmes TC, Dipersio CM, Hynes RO, Su X, Rich A. Self-complementary oligopeptide matrices support mammalian-cell attachment. *Biomaterials*. 1995; 16:1385–1393. [PubMed: 8590765]
47. Hartgerink JD, Beniash E, Stupp SI. Self-assembly and mineralization of peptide-amphiphile nanofibers. *Science*. 2001; 294:1684–1688. [PubMed: 11721046]
48. Larsen TH, Branco MC, Rajagopal K, Schneider JP, Furst EM. Sequence-dependent gelation kinetics of beta-hairpin peptide hydrogels. *Macromolecules*. 2009; 42:8443–8450. [PubMed: 20161466]
49. Zhang SM, Greenfield MA, Mata A, Palmer LC, Bitton R, Mantei JR, Aparicio C, de la Cruz MO, Stupp SI. A self-assembly pathway to aligned monodomain gels. *Nature Mater*. 2010; 9:594–601. [PubMed: 20543836]
50. Petka WA, Harden JL, McGrath KP, Wirtz D, Tirrell DA. Reversible hydrogels from self-assembling artificial proteins. *Science*. 1998; 281:389–392. [PubMed: 9665877]
51. Barati D, Moeinzadeh S, Karaman O, Jabbari E. Time dependence of material properties of polyethylene glycol hydrogels chain extended with short hydroxy acid segments. *Polymer*. 2014; 55:3894–3904. [PubMed: 25267858]
52. Moeinzadeh S, Barati D, He X, Jabbari E. Gelation characteristics and osteogenic differentiation of stromal cells in inert hydrolytically degradable micellar polyethylene glycol hydrogels. *Biomacromolecules*. 2012; 13:2073–2086. [PubMed: 22642902]
53. Moeinzadeh S, Khorasani SN, Ma J, He X, Jabbari E. Synthesis and gelation characteristics of photo-crosslinkable star poly (ethylene oxide-co-lactide-glycolide acrylate) macromonomers. *Polymer*. 2011; 52:3887–3896. [PubMed: 21927508]
54. Posocco P, Fermeglia M, Pricl S. Morphology prediction of block copolymers for drug delivery by mesoscale simulations. *J Mater Chem*. 2010; 20:7742–7753.
55. Odian, G. Principles of polymerization. New York: John Wiley; 1981.
56. Nicolai T, Colombani O, Chassenieux C. Dynamic polymeric micelles versus frozen nanoparticles formed by block copolymers. *Soft Matter*. 2010; 6:3111–3118.
57. Flory, PJ. Principles of polymer chemistry. New York: Cornell University Press; 1953.
58. Peppas NA, Bures P, Leobandung W, Ichikawa H. Hydrogels in pharmaceutical formulations. *Eur J Pharmaceut Biopharmaceut*. 2000; 50:27–46.
59. Cima LG, Lopina ST. Network structures of radiation-crosslinked star polymer gels. *Macromolecules*. 1995; 28:6787–6794.
60. Elliott JE, Bowman CN. Kinetics of primary cyclization reactions in cross-linked polymers: An analytical and numerical approach to heterogeneity in network formation. *Macromolecules*. 1999; 32:8621–8628.
61. Ganji F, Vasheghani-Farahani S, Vasheghani-Farahani E. Theoretical description of hydrogel swelling: A review. *Ir Polym J*. 2010; 19:375–398.

62. Sukumar VS, Lopina ST. Network model for the swelling properties of end-linked linear and star poly(ethylene oxide) hydrogels. *Macromolecules*. 2002; 35:10189–10192.
63. Boonthekul T, Hill EE, Kong HJ, Mooney DJ. Regulating myoblast phenotype through controlled gel stiffness and degradation. *Tissue Eng*. 2007; 13:1431–1442. [PubMed: 17561804]
64. Khetan S, Guvendiren M, Legant WR, Cohen DM, Chen CS, Burdick JA. Degradation-mediated cellular traction directs stem cell fate in covalently crosslinked three-dimensional hydrogels. *Nature Mater*. 2013; 12:458–465. [PubMed: 23524375]
65. Kharkar PM, Kiick KL, Kloxin AM. Designing degradable hydrogels for orthogonal control of cell microenvironments. *Chem Soc Rev*. 2013; 42:7335–7372. [PubMed: 23609001]
66. Nakayama Y, Okuda K, Takamizawa K, Nakayama A. Preparation of well-defined poly(ether-ester) macromers: Photogelation and biodegradability. *Acta Biomater*. 2011; 7:1496–1503. [PubMed: 21095246]
67. Ko CY, Yang CY, Yang SR, Ku KL, Tsao CK, Chuang DCC, Chu IM, Cheng MH. Cartilage formation through alterations of amphiphilicity of poly(ethylene glycol)-poly(caprolactone) copolymer hydrogels. *RSC Adv*. 2013; 3:25769–25779.
68. Rodriguez-Galan A, Franco L, Puiggali J. Degradable poly(ester amide)s for biomedical applications. *Polymer*. 2011; 3:65–99.
69. He JL, Zhang MZ, Ni PH. Rapidly in situ forming polyphosphoester-based hydrogels for injectable drug delivery carriers. *Soft Matter*. 2012; 8:6033–6038.
70. Wang YC, Lee WJ, Ju SP. Modeling of the polyethylene and poly(L-lactide) triblock copolymer: A dissipative particle dynamics study. *J Chem Phys*. 2009; 131:124901. [PubMed: 19791915]
71. Zheng YT, He CL, Huynh CT, Lee DS. Biodegradable pH- and temperature-sensitive multiblock copolymer hydrogels based on poly(amino-ester urethane)s. *Macromol Res*. 2010; 18:974–980.
72. Kloxin AM, Kasko AM, Salinas CN, Anseth KS. Photodegradable hydrogels for dynamic tuning of physical and chemical properties. *Science*. 2009; 324:59–63. [PubMed: 19342581]
73. Cukierman E, Pankov R, Yamada KM. Cell interactions with three-dimensional matrices. *Curr Opin Cell Biol*. 2002; 14:633–639. [PubMed: 12231360]
74. Dalby MJ, Gadegaard N, Oreffo ROC. Harnessing nanotopography and integrin-matrix interactions to influence stem cell fate. *Nature Mater*. 2014; 13:558–569. [PubMed: 24845995]
75. Gloe T, Pohl U. Laminin binding conveys mechanosensing in endothelial cells. *News Physiol Sci*. 2002; 17:166–169. [PubMed: 12136046]
76. Aplin AE, Howe A, Alahari SK, Juliani RL. Signal transduction and signal modulation by cell adhesion receptors: The role of integrins, cadherins, immunoglobulin-cell adhesion molecules, and selectins. *Pharmacol Rev*. 1998; 50:197–263. [PubMed: 9647866]
77. Silva AKA, Richard C, Bessodes M, Scherman D, Merten OW. Growth factor delivery approaches in hydrogels. *Biomacromolecules*. 2009; 10:9–18. [PubMed: 19032110]
78. Zhu JM. Bioactive modification of poly(ethylene glycol) hydrogels for tissue engineering. *Biomaterials*. 2010; 31:4639–4656. [PubMed: 20303169]
79. Liu SQ, Tian QA, Wang L, Hedrick JL, Hui JHP, Yang YY, Ee PLR. Injectable biodegradable poly(ethylene glycol)/rgd peptide hybrid hydrogels for in vitro chondrogenesis of human mesenchymal stem cells. *Macromol Rapid Commun*. 2010; 31:1148–1154. [PubMed: 21590868]
80. Moeinzadeh S, Barati D, Sarvestani SK, Karimi T, Jabbari E. Experimental and computational investigation of the effect of hydrophobicity on aggregation and osteoinductive potential of bmp-2 derived peptide in a hydrogel matrix. *Tissue Eng Part A*. 2014; 21:134–46. [PubMed: 25051457]

- PEG extended with aliphatic hydroxy acid (HA) segment to form degradable gels.
- The HA-chain-extended PEG was soluble in water and formed micellar structures.
- Micelle formation led to gels with tunable degradation from days to months.
- Micelle formation enhanced differentiation of mesenchymal stem cells in gels.

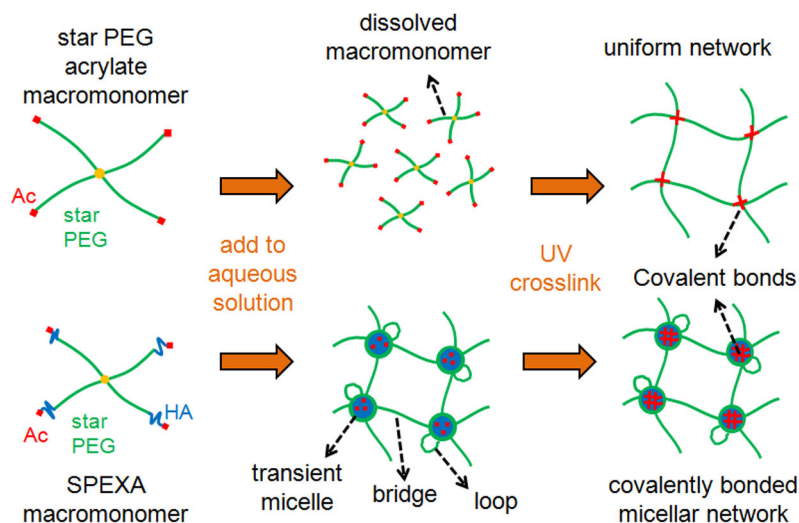
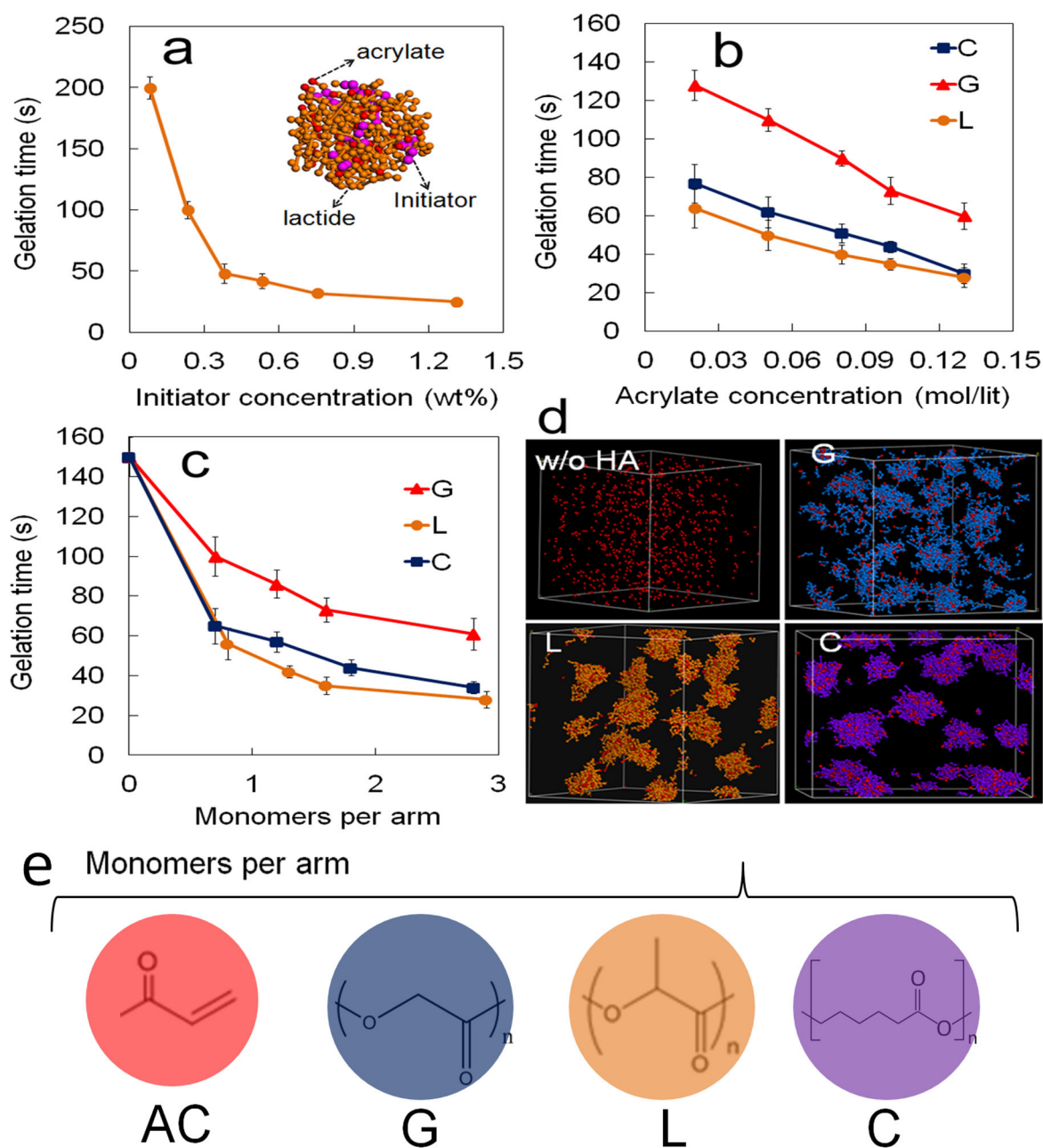


Fig. 1. Schematic representation for the formation of a uniformly crosslinked gel (top) versus a micellar gel (bottom). Green, red and blue colors represent PEG, acrylate (Ac) and aliphatic hydroxy acid (HA), respectively. Star PEG acrylate macromonomers were soluble in aqueous solution in the absence of HA, crosslinked under UV irradiation and formed a uniform network (top). SPEXA macromonomers formed a transient micellar network in aqueous solution due to aggregation of the hydrophobic HA segments and Ac groups. The Ac groups within the micelles' core crosslinked under UV irradiation which transformed the transient micellar network to a permanent covalent-crosslinked micellar gel.

**Fig. 2.**

(a) Effect of initiator concentration on the gelation time of L hydrogel (20 wt%, $m=1.7$), the inset in (a) shows the simulated distribution of initiator molecules in the hydrophobic core of a micelle. The effect of acrylate concentration (b) and number of monomers per macromonomer arm (c) on the gelation time of SPEXA hydrogels. Micelle formation in SPEXA gel precursor solution (20 wt%) and localization of Ac groups within the micelles' core is shown in (d). G, L and C monomers are shown by blue, orange and purple beads, respectively. The chemical structure of Ac, G, L and C groups are shown in (e) (Adapted with permission from refs [30,51,52]).

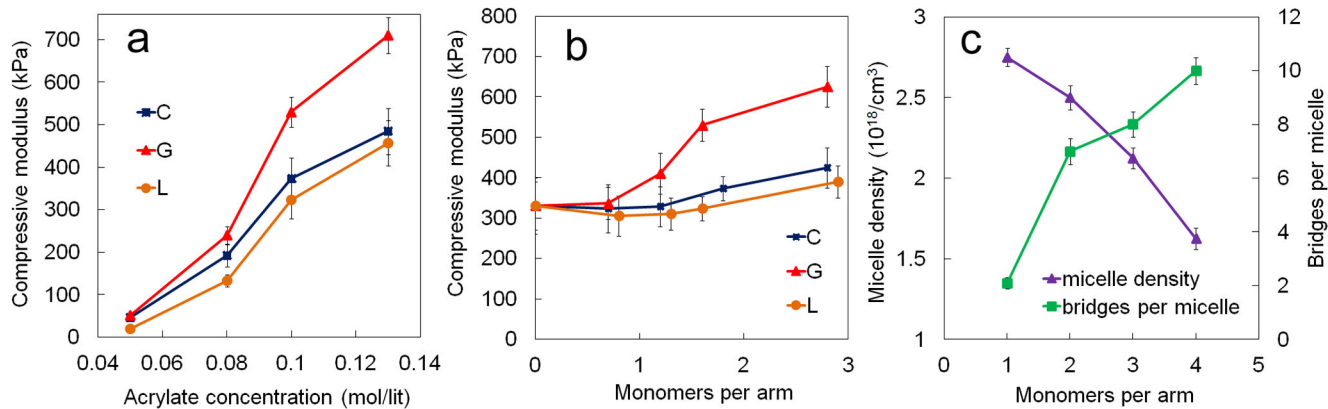


Fig. 3. Effect of acrylate concentration (a) and number of monomers per macromonomer arm (b) on the compressive modulus of SPEXA hydrogels. (c) The simulated effect of number of monomers per macromonomer arm on the number density of micelles and the number of bridges per micelle in the L hydrogel (30 wt%) precursor solution (Adapted with permission from refs [31,51]).

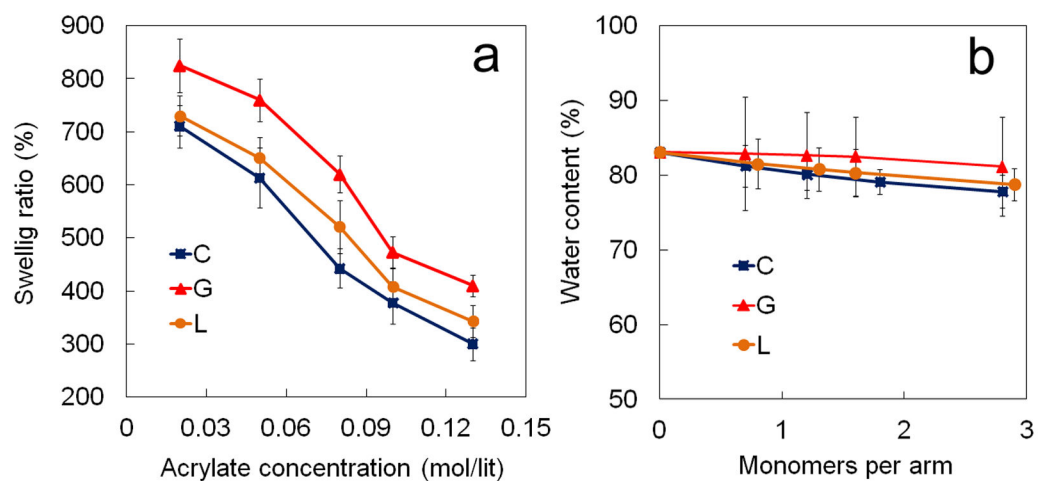


Fig. 4. (a) Effect of acrylate concentration on the swelling ratio of SPEXA hydrogels ($m=1.7$). (b) Effect of number of monomers per macromonomer arm on the water content of SPEXA hydrogels (20 wt%) (Adapted with permission from refs [30,51]).

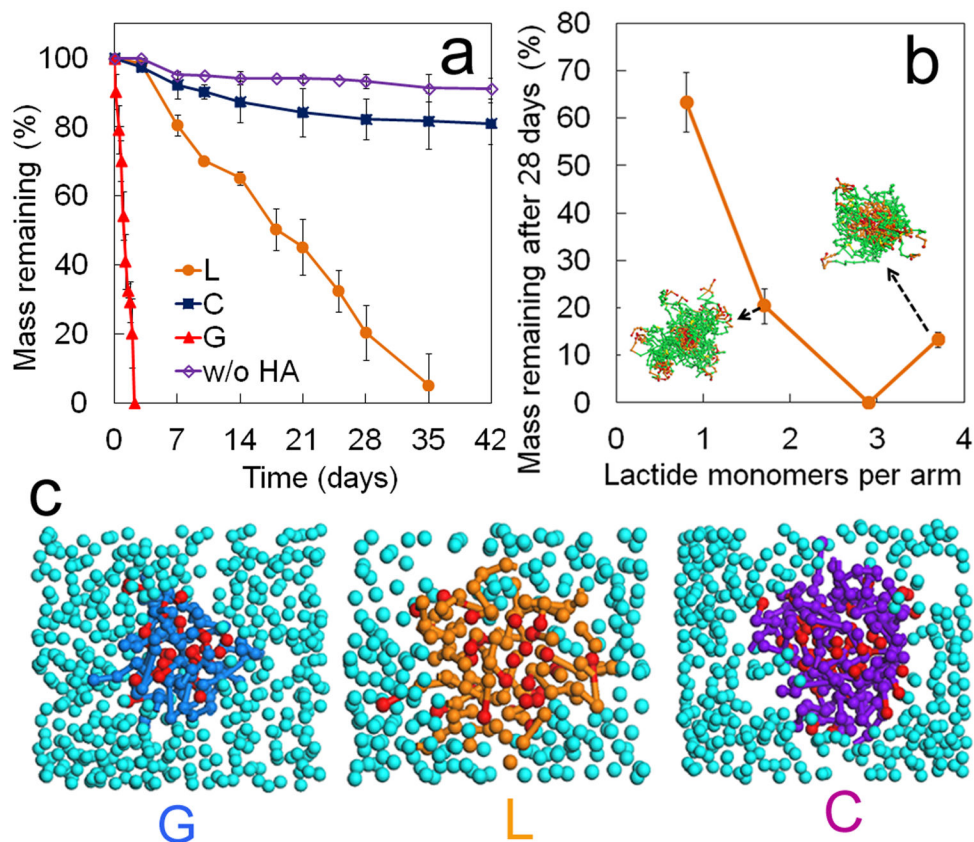


Fig. 5. (a) Effect of HA type on the mass remaining of SPEXA hydrogels (20 wt%, $m=1.7$). (b) Effect of number of L monomers per macromonomer arm on the mass remaining of L hydrogels after 28 days. The insets in (b) are molecular dynamic simulations of the structure of L ($m=1.7$ and 3.7) micelles with green, brown and red beads representing ethylene oxide (EO), lactide and acrylate repeat units in the macromonomer, respectively. (c) Effect of degradable HA monomer type on the distribution of water beads around the micelles' core. G, L, C, Ac, and water units are shown by blue, orange, purple, red, and light blue beads, respectively, and EO beads are not shown for clarity (Adapted with permission from refs [30,52]).

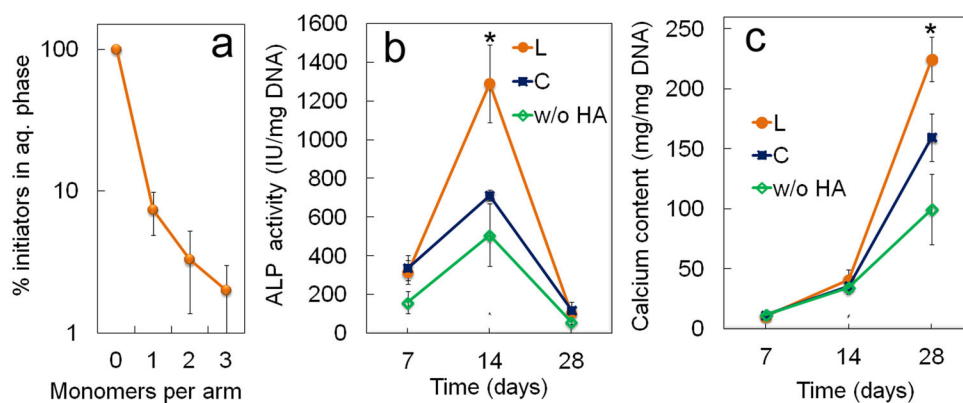


Fig. 6.

(a) Molecular dynamic simulation of the effect of number of degradable lactide monomers per SPEXA macromonomer arm on the fraction of initiator molecules in the aqueous solution of L hydrogel. (b) ALP activity and (c) calcium content of the MSCs encapsulated in SPEXA hydrogels with incubation time in osteogenic medium. A “star” indicates a statically significant difference ($p < 0.05$) between the test group and all other groups at the same time point (Adapted with permission from ref [30]).